ISSN 0208-7774 TRIBOLOGIA 3/2023 p. 31–42
DOI: 10.5604/01.3001.0053.9434

Jaroslaw KACZOR*

SELECTION OF PRELOAD IN TAPERED ROLLER BEARINGS ARRANGEMENT ACCORDING TO DURABILITY CRITERION

DOBÓR ZACISKU WSTĘPNEGO W UKŁADZIE ŁOŻYSK STOŻKOWYCH WEDŁUG KRYTERIUM TRWAŁOŚCI

Key words: tapered roller bearing, preload, shaft loading, durability of bearing, elasticity of bearing.

Abstract: The main purpose of using tapered roller bearings is to obtain high bearing stiffness. High bearing stiffness is achieved by using an appropriate mounting clamp in the bearing system. The mounting clamp, or in other words, the pre-clamp, is currently selected based on experience. The literature lacks precise indications regarding the size of the initial clamp of the bearing arrangement depending on the external load, and it is selected intuitively. The wrong choice of preload can have a disastrous effect on the life of the entire bearing arrangement.
This study aims to determine the maximum preload in the tapered roller bearing system, taking into account its durability and the elasticity of the bearings and the shaft.
In this article, different load variants are analysed, considering the effect of preload on the fatigue life of the bearing system, and recommendations are proposed for the acceptable preload value depending on the size of the bearings used.

Słowa kluczowe: łożysko stożkowe, zacisk występny, obciążenie wału, trwałość łożyskowania, sprężystość łożysk.

Streszczenie: Głównym celem stosowania łożysk stożkowych jest uzyskanie dużej sztywności łożyskowania. Uzyskanie dużej sztywności łożyskowania osiąga się poprzez zastosowanie odpowiedniego zacisku montażowego w układzie łożysk. Zacisk montażowy czy inaczej mówiąc – zacisk wstępny dobierany jest obecnie w oparciu o doświadczenie. W literaturze brakuje dokładnych wskazówek dotyczących wielkości zacisku wstępnego układu łożysk w zależności od obciążenia zewnętrznego i jest on dobierany intuicyjnie. Zły dobór zacisku wstępnego może mieć katastrofalny wpływ na trwałość całego układu łożyskowego.
Celem tej pracy jest określenie maksymalnego napięcia wstępnego w układzie łożysk stożkowych, biorąc pod uwagę jego trwałość przy uwzględnieniu sprężystości łożysk oraz sprężystości wału.
W artykule przeanalizowano różne warianty obciążenia z uwzględnieniem wpływu napięcia wstępnego na trwałość zmęczeniową układu łożyskowego oraz zaproponowano zalecenia dotyczące dopuszczalnej wartości napięcia wstępnego w zależności od rozmiaru zastosowanych łożysk.

INTRODUCTION

In modern scientific literature, much information can be found concerning the effect of preload on bearings and bearing systems. The preload is applied not only in the case of angular contact ball bearings but also in the case of other bearings, e.g. **[L. 1]** presents a generalisation of previous works developed by the authors in the field of calculation and selection of slewing bearings where a theoretical model for the estimation of the static load-carrying capacity of four-contact-point slewing bearings was obtained. In those previous works, it was assumed that there was no preload in the balls; in the work presented, the model has been improved in order to consider the effect of the preload in such a way that it provides more realistic results because this type of bearings is preloaded in several applications to increase the stiffness and therefore the accuracy of the system. In parallel and

* ORCID: 0000-0003-2315-980X. Technical University of Lodz, Institute of Sanitary Engineering and Building Installations, Żeromskiego 116 Street, 90-924 Łódź, Poland

for comparison purposes, the finite element model built by the authors in previous works has also been adapted to include the preload in the balls. This **[L. 2]** presents the results of experimental studies on the effects of mechanical preload and bearing clearance on the rotordynamic performance of lobed gas foil bearings (GFBs) for oil-free turbochargers (TCs).

Great attention was paid to the effect of the preload on the stiffness of machine tool spindles in relation to thermal effects, e.g. **[L. 3]** presents a unified method to predict nonlinear thermal characteristics of a high-speed spindle bearing subjected to a preload. Based on a quasi-static model and different finite methods, the change of thermal contact resistance, bearing parameters and heat source with temperature per second is completely analysed using a new algorithm. The bearing parameters and lubricant viscosity, affected by time-varying temperature, are updated in each time step. As a result, the thermal effects on contact angles, contact forces, the preload and stiffness of the bearing are found. Moreover, our analysis results show that the estimated preload and bearing stiffness nonlinearly vary with the increase in temperature, and the presented method takes much less computational effort than the finite element method. In **[L. 4]**, a multi-objective optimisation is performed for the design of a spindle-bearing system based on particle swarm optimisation (PSO). Multiple objectives, such as natural frequencies, static stiffness and total friction torque, are considered in this design optimisation. Bearing preload and bearing locations are selected as the design variables. Pareto-optimal solutions are used to support the selection of optimal values of the design parameters. A finite element model is established to analyse and design the spindle system with four angular contact ball bearings.

Then in **[L. 5]**, the effects of preload and preload method on the rotational performance of the spindle-bearing system are explored experimentally to reveal the role of preload and preload method in spindle rotational performances under different speeds are presented.

The preload of the angular contact ball bearing is extremely important according to the following: high speed of the spindle greatly influences the spindle's dynamic and thermal characteristics **[L. 6]**, vibrations **[L. 7]**, the performance of the spindle system and bearings in a machine tool **[L. 8**, **9]**, dynamic characteristics of a rotor **[L. 10]**, on the dynamic performance of the bearing system **[L. 11]** and spindles **[L. 12]**. In **[L. 11]**, the maximum compliance of the spindle tool tip occurred at the spindle shaft's bending vibrations and varied with the preload amount on a spindle's bearing.

The preload significantly affects the axial stiffness of the machine tool spindle, as shown in **[L. 13**, **14]**, where the axial stiffness softening and hardening characteristics of the machine tool spindle are studied. "The results show that when a bearing preload reaches a certain relatively large threshold, a "sag" shape occurs in the axial stiffness curve, indicating the "stiffness hardening" characteristic of the spindle. On the other hand, for a small preload, no "sag" shape occurs in the spindle stiffness curve, indicating a "stiffness softening" characteristic of the spindle. This phenomenon is significant for acquiring excellent spindle stiffness properties" **[L. 13]**.

The wear between the balls and races significantly affects the bearing's dynamic characteristics, which is the main cause of bearing failure. Some existing contact stiffness models were established to study the dynamic characteristics of bearings **[L. 15]**. However, bearing wear has rarely been investigated due to the contact load and wear mechanism complexities.

CALCULATION METHOD

The life of the angular contact bearing system can be determined to a good approximation using the catalogue method. However, this method is unsuitable for calculations that consider the influence of preload. Therefore in the presented work, a method based on the value of the average shaft load (rolling element) **[L. 16**, **17**, **18**, **19**, **20]** is used.

It is impossible to determine forces acting in bearings if the elasticity of bearings and shaft are not considered simultaneously. The bearings and the shaft are coupled systems in which a shaft deflection forces an angular deflection of the bearing rings but the angular deflection of the bearing rings causes a reaction torque in the bearings (except for self-aligning bearings).

This reaction torque impacts reducing the shaft deflection. A preload must be applied, i.e., closing up the outer bearing rings towards each other. This clamp will manifest itself as the sum of

axial deflections in both bearings, but it is unknown beforehand how this sum is distributed between the two bearings of the arrangement.

The influence of the following factors on the rolling element load in the bearing was therefore considered:

- radial and axial load acting on the bearing shaft,
- elastic deflection of the shaft causing deflection of the inner bearing rings,
- preload.

The exact solution to the problem is presented in works **[L. 21**, **22]**.

CALCULATION EXAMPLE

Taper roller bearings of the basic type, i.e. series 302, were used as the calculation subject. Bearing No. 30209 was selected for the calculation example. The dimensions of the bearings' work surfaces are required for the calculation. They were assumed according to the archival documentation of CBKŁT. There were no contemporary data available regarding this topic (bearing manufacturers keep these dimensions as production secrets), but contemporary deviations from these archival data cannot be very big (overall dimensions of bearings are unchangeable). Therefore these possible deviations cannot qualitatively influence calculation results. Dimensions of the work surfaces of selected bearings are shown in **Table 1**.

A model shaft was determined for the selected bearings, the dimensions of which are defined according to **Figure 1** and given in **Table 2**. It was assumed that two identical tapered roller bearings support the shaft in an X arrangement in each calculation case.

Table 1. Dimensions of work surfaces of bearings taken into account for calculation
Tabela 1. Wymiary powierzchni roboczych łożysk przyjętych do obliczeń

Bearing →	30206	30209	30212	30224
D_k [mm]	6.137	10.495	13.491	24.907
L_n [mm]	12.2	13.8	15.5	30.3
r_e [mm]	108	150	193	356
s_r [mm]	0.3	0.5	0.5	1
Z	17	19	19	20
D_1 [mm]	40.632	57.945	74.485	150.478
r_{bz} [mm]	6000	7500	11500	28900
α [rad]	0.244976	0.2637096	0.2637096	0.2822585
δ [rad]	1.562070	1.562070	1.562070	1.562070
β [rad]	0.0349066	0.0349066	0.0349066	0.0349066

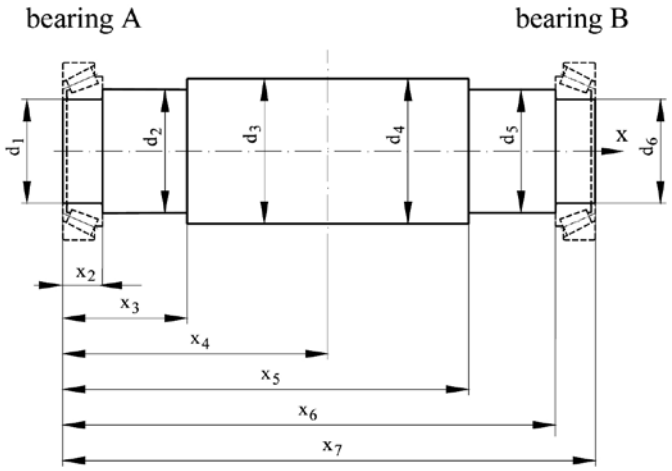

Fig. 1. Model shaft design
Rys. 1. Szkic modelowego wału

Table 2. Dimension parameters of models shafts [mm]
Tabela 2. Parametry wymiarowe modelowych wałów [mm]

Bearing →	30206	30209	30212	30224
x_2	17	21	24	44
x_3	50	75	100	200
x_4	100	150	200	400
x_5	150	225	300	600
x_6	183	279	376	756
x_7	200	300	400	800
d_1	30	45	60	120
d_2	36	52	69	135

The shape of the shaft was selected according to the typical shape of gear shafts in which the bearings are placed at the ends of the shaft, and the diameters at the individual segments correspond to the theoretical outline being built on the principle of equal bending strength. In technical reality, there are infinitely many types of shaft shapes.

The shaft beginning coordinate x1 was assumed to be equal to zero for all model shafts.

The bearing was calculated with loads varying in value. A variant of the load location is shown in **Figure 2**.

The loading forces (circumferential, radial and axial) are applied at points determined by a straight line running through the wheel parallel to the 'z' axis; thus, circumferential forces F_c are directed parallel to the 'y' axis, radial forces F_p are directed towards the centre of the wheel, axial forces F_x are parallel to the 'x' axis. The location of the load application points is defined by angles β1 and β2. The directions of the radial and axial forces are defined in the same way as in the figure.

Locations of load planes were assumed in fixed relations to the shaft length L_w, equal to dimension x_7 from **Table 2**:

For location variant I:
$x_L = 0.4\ L_w$, or $x_L = 0.5\ L_w$ or $x_L = 0.6\ L_w$.
For placement variant II:
$x_{L1} = 0.4\ L_w$, $x_{L2} = 0.6$ Lw.
Rolling wheel diameter $D_t = 150$ mm.
The loads presented in **Figure 13** are assumed to be identical ($F_{c1} = F_{c2}$, $F_{p1} = F_{p2}$, $F_{x1} = F_{x2}$).

Firstly, it was established that the circumferential force on the alleged Fc1 gear wheel would be taken at three levels: 0.075 dynamic load capacity C, 0.1 dynamic load capacity C or 0.125 dynamic load capacity C **[L. 23]**.

Assuming that the interlocking buttress angle of the gears is 20º, the radial Fp force was set as approximately 0.36 of the circumferential force. The axial F_x force was assumed in five values in the following fixed relations to the circumferential force, similar to previous ball bearings calculations.

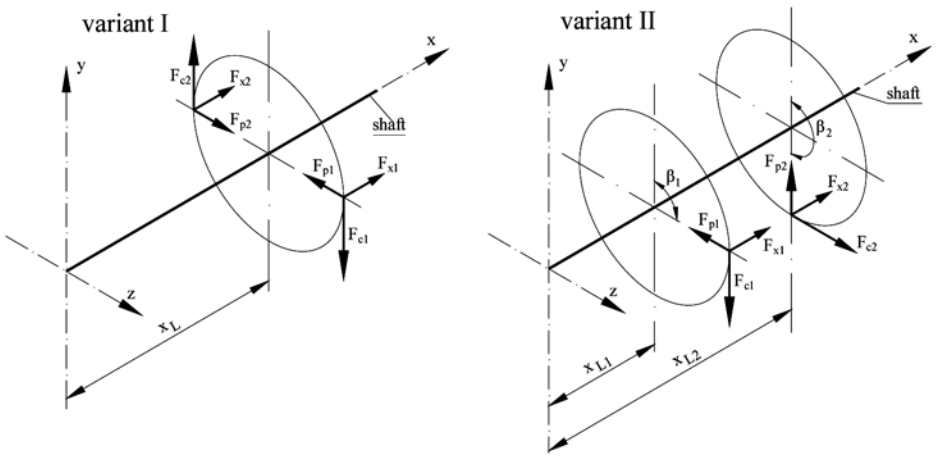

Fig. 2. Assumed bearing load variants
Rys. 2. Przyjęte warianty obciążenia łożyskowania

However, due to the greater weight of the axial force in tapered roller bearings than in angular contact ball bearings, the axial force contributions were reduced accordingly. This was done on the principle of inverse proportionality to the thrust load Y factor. In the tapered roller bearings of the 302 series – slightly more than 1.4. Therefore, the axial force's contribution was assumed smaller for the tapered roller bearings in the ratio 0.57:1.4 = 0.41.

Hence the following relative values of the axial forces for the tapered roller bearings of 302 series resulted: 0, 0.03 F_c, 0.05 F_c, 0.0874 F_c, 0.16 F_c. Since in the assumed load variant, two equal axial forces and two equal circumferential forces act on the bearing, the ratio of the sum of axial forces to the sum of circumferential forces is described by the same series of numbers. The circumferential F_c force is not the only transverse load (the other one is the radial force). However, due to the assumed constant ratio of the radial force to the circumferential one, it is assumed to treat the ratio of the circumferential force to the bearing F_c/C carrying capacity as a parameter characterising the level of the transverse load in the bearing arrangement.

The load values summarised in **Table 3** result from the above findings.

Table 3. Load values assumed for calculation
Tabela 3. Przyjęte do obliczeń wartości obciążeń

Bearing		30206			30209			30212			30224		
F_c/C		0.075	0.100	0.125	0.075	0.100	0.125	0.075	0.100	0.125	0.075	0.100	0.125
F_c [N]		3015	4020	5025	4950	6600	8250	7425	9900	12375	25575	34100	42625
F_p [N]		1097	1463	1830	1802	2402	3003	2703	3600	4500	9310	12410	15520
F_x [N]	1	0	0	0	0	0	0	0	0	0	0	0	0
	2	90	121	151	149	198	248	223	297	371	768	1023	1279
	3	151	201	251	248	330	413	371	495	619	1279	1705	2131
	4	264	351	439	433	577	721	649	865	1082	2235	2980	3725
	5	482	643	804	792	1056	1320	1188	1584	1980	4092	5456	6820

CALCULATION RESULTS

First, the influence of the initial clamp on the durability of the bearing 'A' and 'B' was determined, where it was found that the life of one bearing decreased while the other increased. From the performed observation, it was not possible to unequivocally state what value of the initial clamp is optimal for the bearing system. Therefore, the characteristics of the W_T index, combining the durability of both bearings, were determined.

$$W_T = \frac{L_{hA}}{L_{hA0}} \cdot \frac{L_{hB}}{L_{hB0}}$$

where:
L_{hA} – fatigue life of the bearing A determined in specific conditions with applied preload,
L_{hB} – fatigue life of the bearing B determined in the same conditions with applied preload,
L_{hA0} – fatigue life of the bearing A determined in specific conditions without preload,
L_{hB0} – fatigue life of the bearing B determined in the same conditions without preload.

The W_T index is an overall parameter that applies to the simultaneous operation of both bearings. Therefore, the formulation of this indicator made it possible to observe the life of the complete bearing system.

The second important advantage of the indicator formulated in this way is that when the life of one of the bearings drastically decreases (e.g., close to zero), the indicator's value also decreases close to zero. Moreover, an increase in the life of both bearings causes an increase in this indicator, and a decrease in one causes a decrease. Therefore, it gives a correct evaluation of the bearing life as a whole.

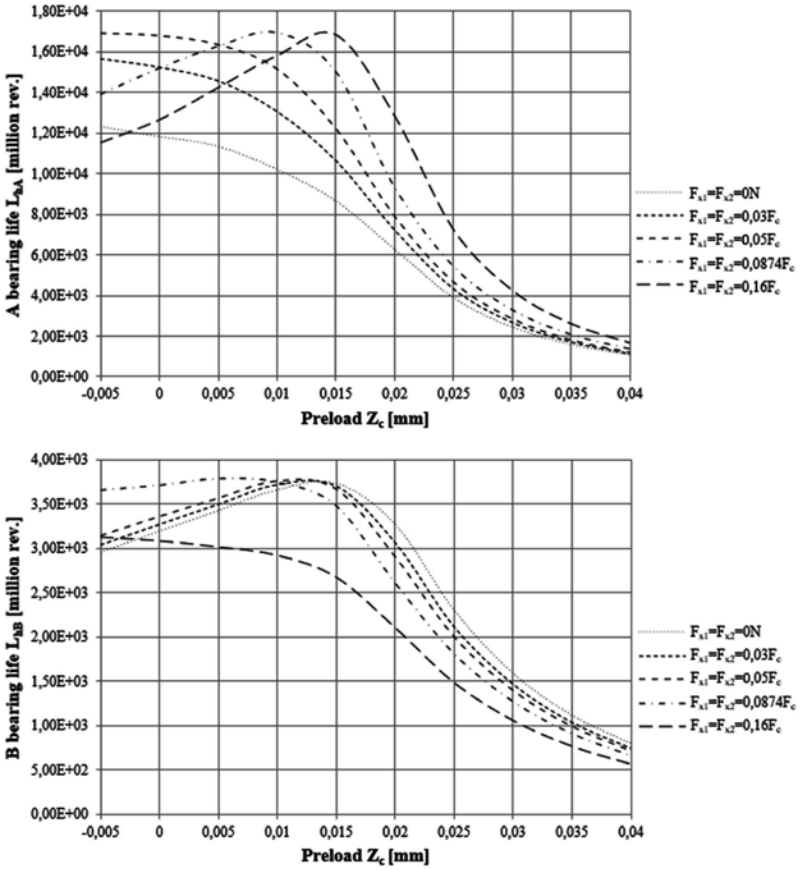

Fig. 3. Life of 'A' and 'B' bearing for the circumferential load, which is 0,075C for bearing 30209
Rys. 3. Trwałość łożyska „A" i „B" dla obciążenia obwodowego wynoszącego 0,075C dla łożyska 30209

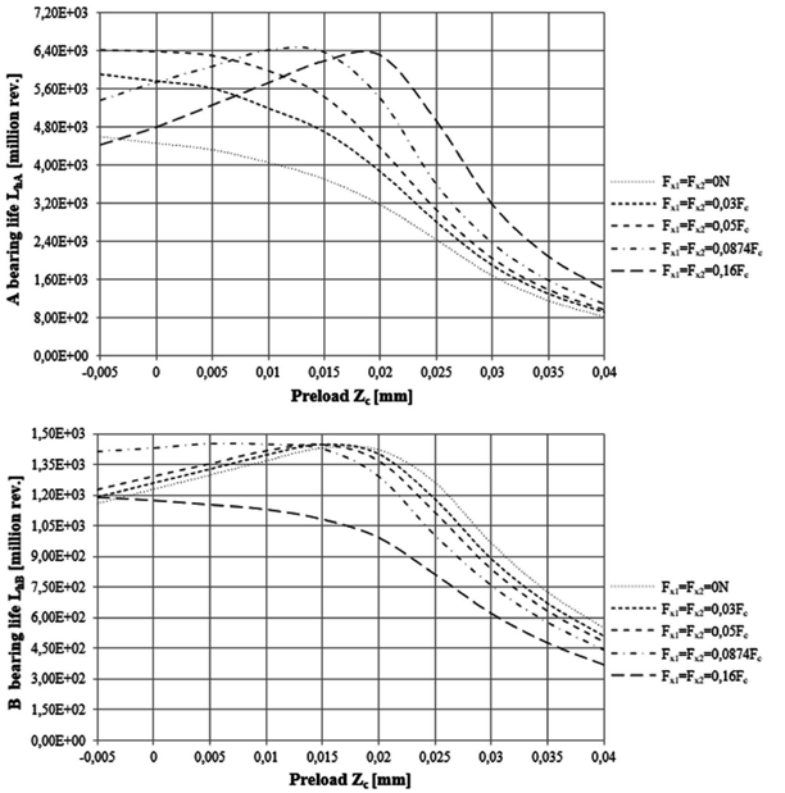

Fig. 4. Life of 'A' and 'B' bearing for the circumferential load, which is 0,1C for bearing 30209
Rys. 4. Trwałość łożyska „A" i „B" dla obciążenia obwodowego wynoszącego 0,1C dla łożyska 30209

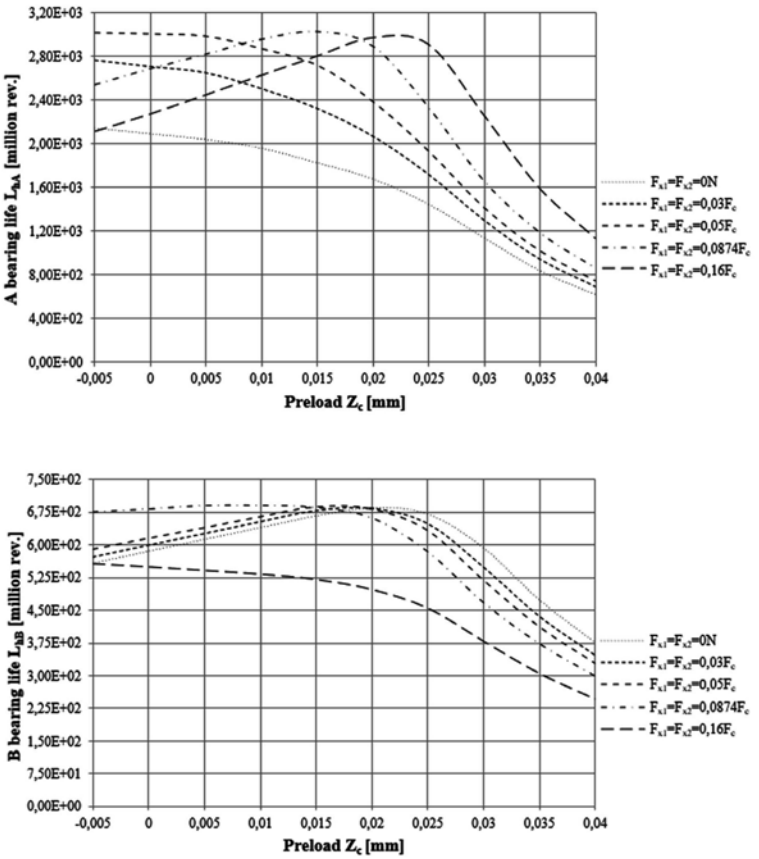

Fig. 5. Life of 'A' and 'B' bearing for the circumferential load, which is 0,125C for bearing 30209
Rys. 5. Trwałość łożyska „A" i „B" dla obciążenia obwodowego wynoszącego 0,125C dla łożyska 30209

Figs 3–5 show example characteristics of fatigue life of left (A) and right (B) bearings as a function of preload Zc for assumed load values and the bearing version 30209 for one design variant and load plane $x_L = 0.6$ Lw.

Examples of W_T index characteristics for bearing 30209 and for the adopted load values are shown in **Figure 6**.

In order to determine a beneficial range of preload, summary graphs based on agreed boundary points were developed. The agreed boundary points were the values Z_c, for which characteristics of the W_T indicator have the value 0.98. It has been arbitrarily assumed that, in order to increase the longitudinal stiffness of the bearing arrangement, a decrease in the durability index by 2% may be allowed.

Collective diagrams of preload are shown in **Figure 7.** Each of the cumulative diagrams $Z_c = f(F_x / F_c)$ is made for the assumed location of the shaft load and for one type of bearing number and shows the highest value of the initial clamp (limit according to the criterion of $W_T \geq 0.98$) that can be used with the parameters mentioned above in depending on the relative radial load of the bearing arrangement F_c / C and the relative axial force F_x / F_c.

With reference to the load plane position $x_F = 0.6\ L_w$ (**Figure 7**), it can be observed that near the left edge of the diagram, the characteristic curves decrease a little, but from the value of the relative axial load about 0.03÷0.04 they begin to increase. The values of permissible clamping are proportional to both radial load and bearing size. For the mean of the bearings analysed, i.e. 30212, the lowest line runs from the value of 14 μm to the value of 22 μm, so at a slightly lower level than previously recorded.

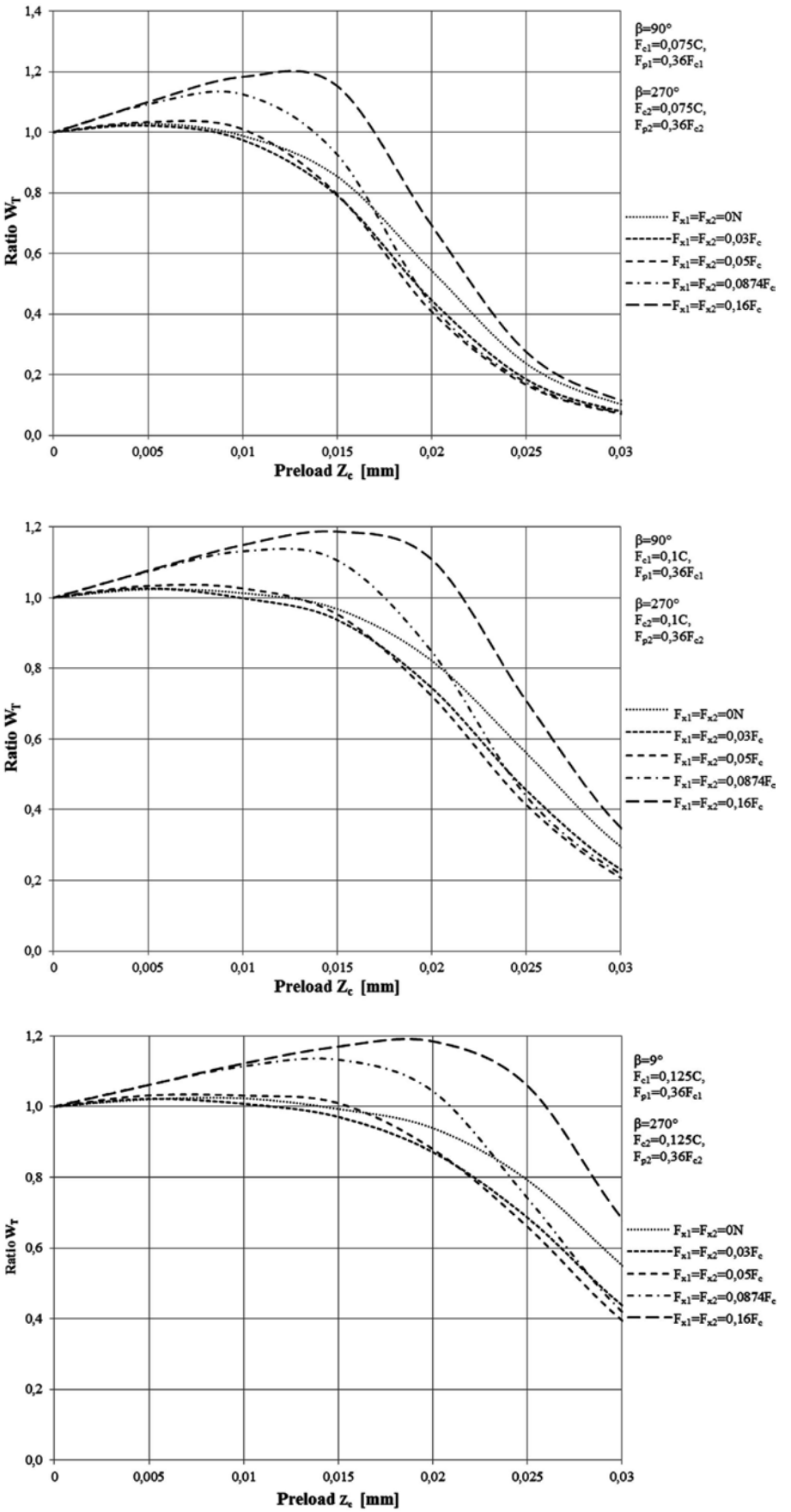

Fig. 6. Example characteristics of the W_T index for the adopted load variant and bearing 30209
Rys. 6. Przykładowa charakterystyka wskaźnika W_T dla przyjętego wariantu obciążenia i łożyska 30209

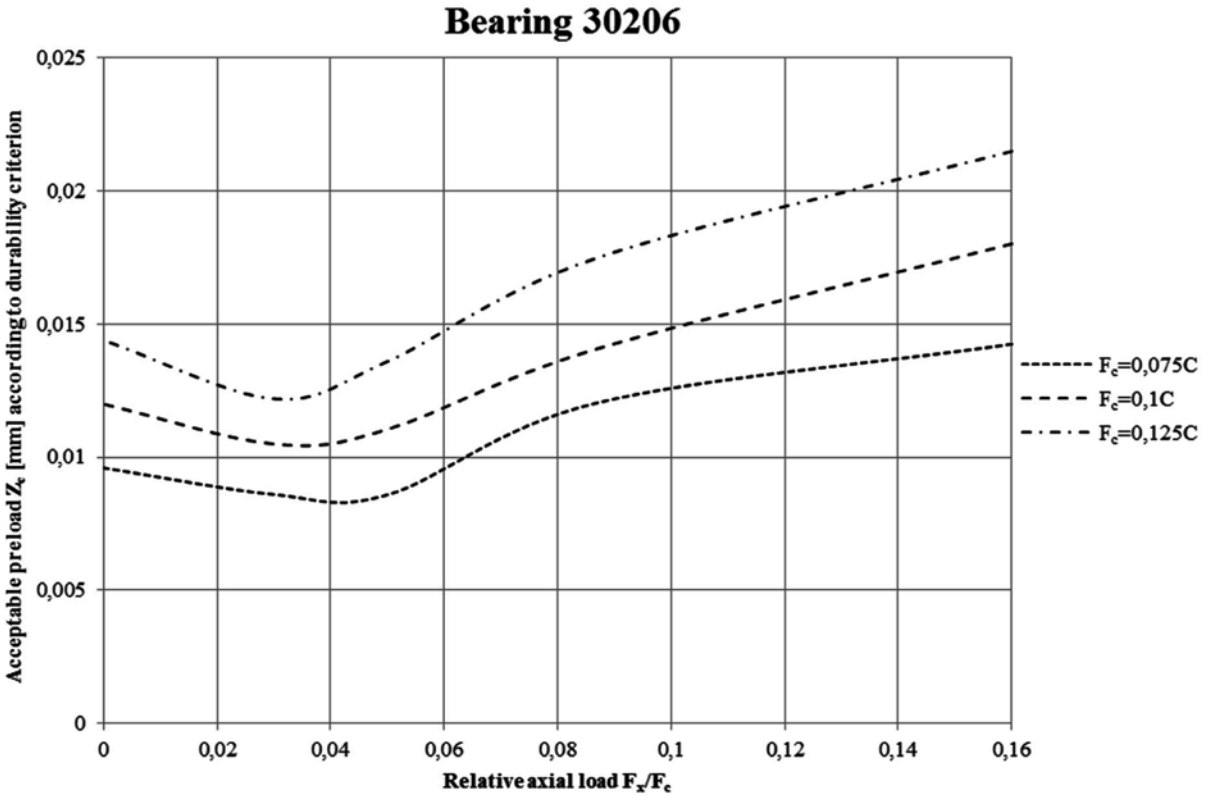
Bearing 30206
Acceptable preload Z_e [mm] according to durability criterion
0,025
0,02
0,015
0,01
0,005
0
0
0,02
0,04
0,06
0,08
0,1
0,12
0,14
0,16
Relative axial load F_x/F_c
F_e=0,075C
F_e=0,1C
F_e=0,125C

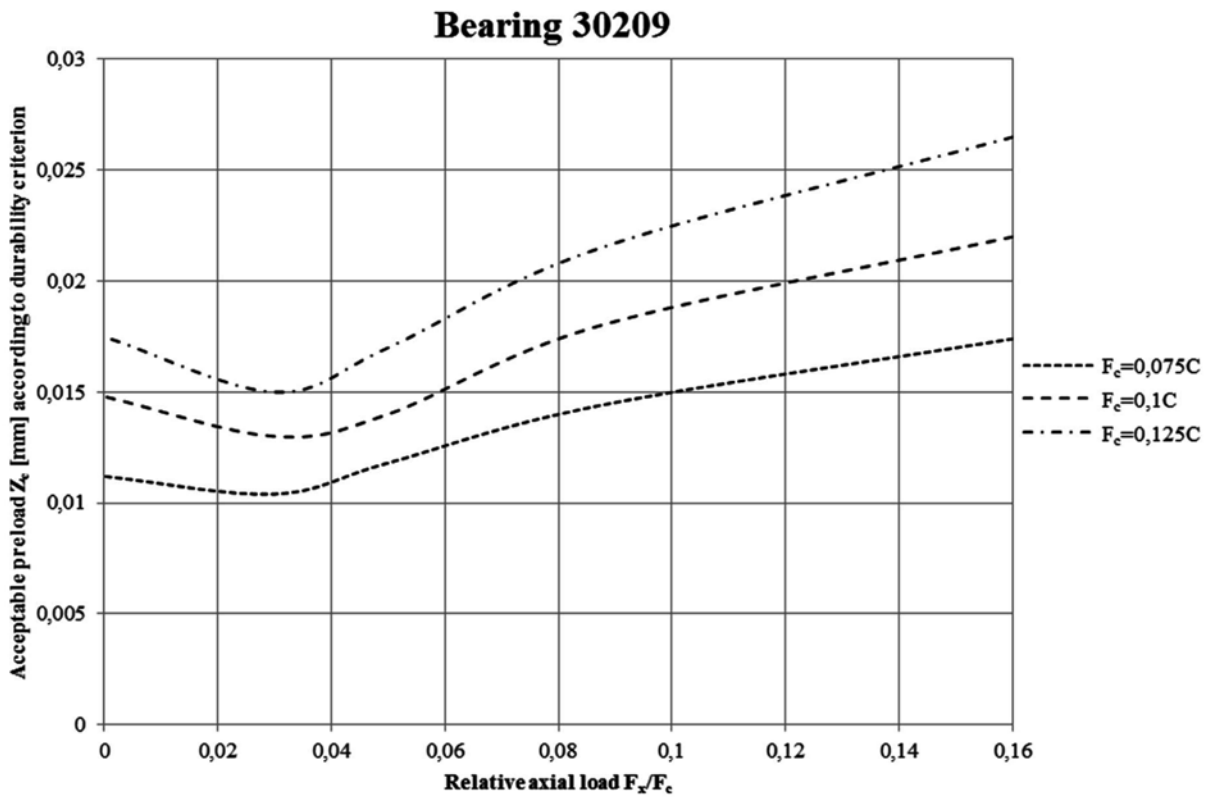
Bearing 30209
Acceptable preload Z_e [mm] according to durability criterion
0,03
0,025
0,02
0,015
0,01
0,005
0
0
0,02
0,04
0,06
0,08
0,1
0,12
0,14
0,16
Relative axial load F_x/F_c
F_e=0,075C
F_e=0,1C
F_e=0,125C

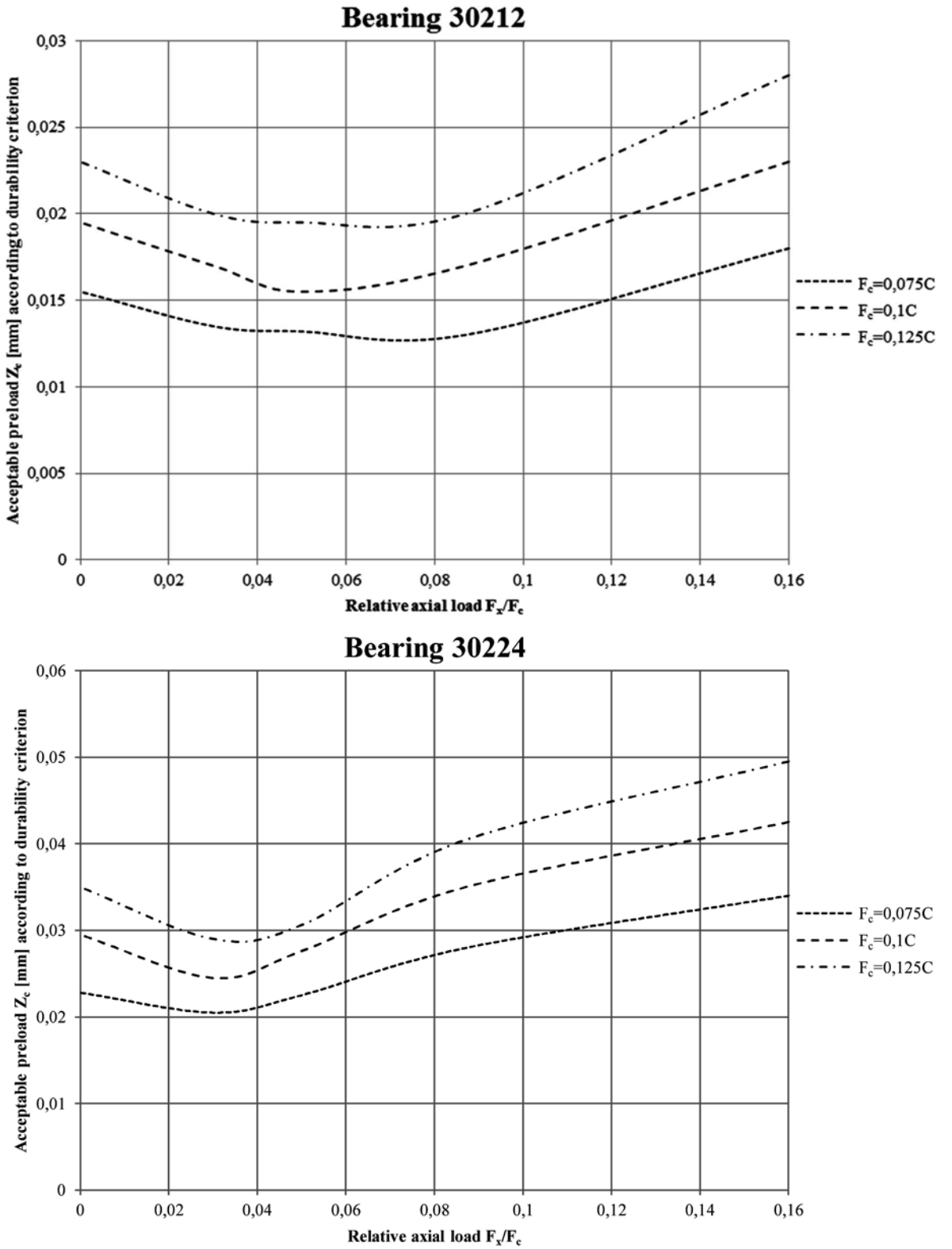

Fig. 7. Acceptable preload Z_c according to durability criterion in the function of relative axial load F_x/F_c for the adopted example

Rys. 7. Dopuszczalny zacisk wstępny Z_c wg kryterium trwałości w funkcji względnego obciążenia osiowego F_x/F_c dla przyjętego do analizy przykładu

CONCLUSION

After additionally analysing other load variants and after taking into account the influence of initial clamping on the bearing stiffness and fatigue life, it can be concluded that the use of initial clamping is beneficial in each case of loading the tapered roller bearing system. The recommendation for an acceptable preload value is based on the most restrictive results. The characteristics of the permissible clamp were built on the most limiting results based on the points corresponding to F_c / C = 0.1 and F_x / F_c = 0. The characteristics thus created are shown in **Figure 8**.

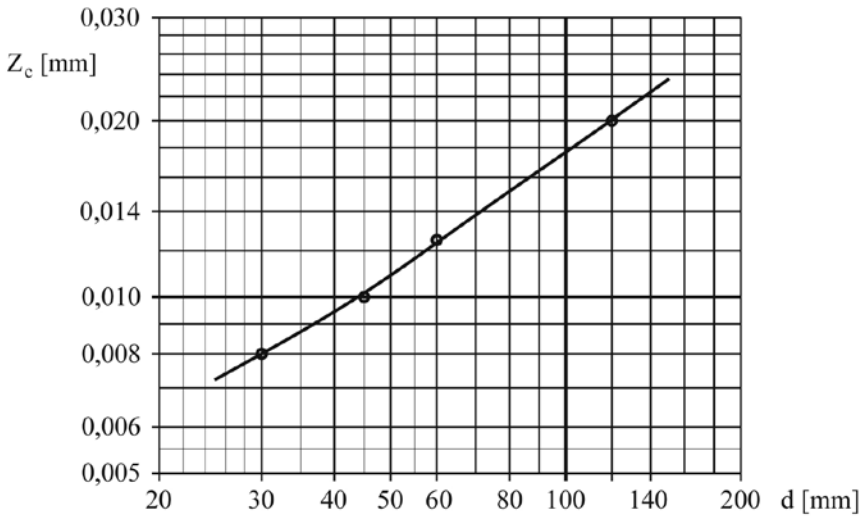

Fig. 8. The dependence of the permissible initial clamp on the bearing diameter according to the durability index criterion
Rys. 8. Zależność dopuszczalnego zacisku wstępnego od średnicy łożyska wg kryterium wskaźnika trwałości

REFERENCES

1. Aguirrebeitia J., Plaza J., Abasolo M., Vallejo J.: Effect of the preload in the general static load-carrying capacity of four-contact-point slewing bearings for wind turbine generators: theoretical model and finite element calculations, Wind Energy 2014, Vol. 17, Issue 10, pp. 1605–162.
2. Chi-Hyuk Ch., Choon-Man L.: A variable preload device using liquid pressure for machine tools spindles, International Journal of Precision Engineering and Manufacturing 2012, 13(6), pp. 1009––1012.
3. Changqing B., Hongyan Z., Xu Qingyu X.: Effects of axial preload of ball bearing on the nonlinear dynamic characteristics of a rotor-bearing system, Nonlinear Dynamics: International Journal of Nonlinear Dynamics and Chaos in Engineering Systems 2008, 53(3), pp. 173–190.
4. Cao H., Holkup T., Altintas Y.: A comparative study on the dynamics of high speed spindles with respect to different preload mechanisms, The International Journal of Advanced Manufacturing Technology 2011, 57(9–12), pp. 871–883.
5. Hongchuan C., Yimin Z., Wenjia L., Yang Z.: Research on the effect of structural and material parameters on vibrations based on quasi-static model of bearings, Journal of the Brazilian Society of Mechanical Sciences and Engineering 2020, 42(11).
6. Hu G., Gao W., Chen Y., Zhang D., Tian Y., Zhang H.: An experimental study on the rotational accuracy of variable preload spindle-bearing system, Advances in Mechanical Engineering 2018, Vol. 10, Issue 5, pp. 1–14.
7. Jianguo G., Yimin Z., Haiyang L.: Influences of wear on dynamic characteristics of angular contact ball bearings, Meccanica: An International Journal of Theoretical and Applied Mechanics AIMETA 2019, 54(7), pp. 945–965.

8. Gaofeng H., Dawei Z., Weiguo G., Ye Ch., Teng L., Yanling T.: Study on variable pressure/position preload spindle-bearing system by using piezoelectric actuators under close-loop control, International Journal of Machine Tools and Manufacture 2018, 125, pp. 68–88.
9. Jui-Pin H., Yuan-Lung L., Tzuo-Liang L., Hsin-Chuan S.: Analysis of the machining stability of a milling machine considering the effect of machine frame structure and spindle bearings: experimental and finite element approaches, The International Journal of Advanced Manufacturing Technology 2013, 68(9–12), pp. 2393–2405.
10. Young-Kug H., Choon-Man L.: A review on the preload technology of the rolling bearing for the spindle of machine tools, International Journal of Precision Engineering and Manufacturing 2010, 11(3), pp. 491–498.
11. Kyuho S., Yong-Bok L.: Effects of Mechanical Preload and Bearing Clearance on Rotordynamic Performance of Lobed Gas Foil Bearings for Oil-Free Turbochargers, Tribology Transactions 2013, Vol. 56, Issue 2, pp. 224–235.
12. Young-Kug H., Choon-Man L.: Development of a simple determination method of variable preloads for high speed spindles in machine tools, International Journal of Precision Engineering and Manufacturing 2015, 16(1), pp. 127–134.
13. Dong Hyeon K., Choon Man L.: A study on the development of a new conceptual automatic variable preload system for a spindle bearing, The International Journal of Advanced Manufacturing Technology 2013, 65(5–8), pp. 817–824.
14. Jinhua Z., Bin F., Yongsheng Z.: A comparative study and stiffness analysis of angular contact ball bearings under different preload mechanisms, Mechanism & Machine Theory 2017, Vol. 115, pp. 1–17.
15. Jiandong L., Yongsheng Z., Ke Y., Xiaoyun Y., Yuwei, L., Jun H.: Research on the axial stiffness softening and hardening characteristics of machine tool spindle system, International Journal of Advanced Manufacturing Technology 2018, 99 (1–4), pp. 951–963.
16. Kaczor J.: Analysis of the influence of shaft load on the value of acceptable preload in a system of angular ball bearings, Tribologia 2020, 290 (2), pp. 25–35.
17. Kaczor J., Raczynski A., The influence of preload on the work of angular contact ball bearings, Archive of Mechanical Engineering 2016, Vol. 63, Issue 3, pp. 319–336.
18. Kaczor J.: Analysis of influence of the load plane combined with preload on durability of bearing, Mechanical Engineering in Transport, Communications 2022, 24, 3, pp. 170–188.
19. Kaczor J., Raczynski A.: The effect of preload of angular contact ball bearings on durability of bearing system. Proceedings of the Institution of Mechanical Engineers, Part J: Journal of Engineering Tribology 2015, Vol. 229, pp. 6723–732.
20. Dong Hyeon K., Choon Man L.: A study on the development of a new conceptual automatic variable preload system for a spindle bearing, The International Journal of Advanced Manufacturing Technology 2013, 65(5–8), pp. 817–824.
21. Kaczor J., Determination of tapered roller bearing system life index considering bearings preload and shaft stiffness, Tribologia – Finnish Journal of Tribology 2022, 39 (1–2).
22. Kaczor J., Effect of tapered roller bearings preload on bearing system durability, Tribologia 2022, pp. 298 (4).
23. CATALOG SKF 1991.